EUROPEAN ORGANIZATION FOR NUCLEAR RESEARCH

CERN-EP/85-74
14 May 1985

REAL-TO-IMAGINARY RATIO OF THE $\bar{p}p$ FORWARD ELASTIC-SCATTERING AMPLITUDE IN THE MOMENTUM RANGE BETWEEN 180 AND 590 MeV/c

W. Brückner, H. Döbbeling, F. Güttner[a)], D. von Harrach, H. Kneis, S. Majewski[a,1)], M. Nomachi[a)], S. Paul, B. Povh, R.D. Ransome, T.-A. Shibata[a)], M. Treichel and Th. Walcher

Max-Planck-Institut für Kernphysik, Heidelberg, Fed. Rep. Germany
Physikalisches Institut der Universität, Heidelberg, Fed. Rep. Germany[a)]

ABSTRACT

The real-to-imaginary ratio of the $\bar{p}p$ forward elastic-scattering amplitude has been measured at the LEAR facility of CERN by the Coulomb–nuclear interference method at seven beam momenta between 181 and 590 MeV/c. The ratio is positive at 590 MeV/c, becomes negative below 500 MeV/c, reaches a minimum at 260 MeV/c, and then crosses zero again at about 230 MeV/c.

(Submitted to Physics Letters B)

---

a) Supported by the Bundesministerium für Forschung und Technologie, Bonn, Fed. Rep. Germany.

1) Present address: FNAL, Batavia, Ill., USA.

1. INTRODUCTION

The measurement of the real-to-imaginary ratio of the $\bar{p}p$ forward elastic-scattering amplitude, ϱ = Re f(t = 0)/Im f(t = 0), is interesting for two reasons. First, it is an important ingredient in dispersion relation calculations. Grein [1] and Kaseno [2] used the ϱ-values at 700 MeV/c [3] and at higher momenta, and showed that a pole in the unphysical region (below the $\bar{p}p$ threshold) was required in order to reproduce the turnover of ϱ to small values at around 700 MeV/c. Iwasaki et al. [4, 5] extended the measurement of the ϱ-value down to 410 MeV/c. They fitted the mass of the pole to their data and derived a value of 1864 ± 12 MeV. Large negative ϱ-values, $\varrho < -0.5$, were extrapolated below 300 MeV/c from their data [4, 5] using this pole in the dispersion relation. Data of two other experiments [6, 7] show nearly the same tendency.

The second point of interest is the question of resonances or baryonium around the threshold [8]. If these resonances would be broad or would sit on a large non-resonant background, they might be visible more sensitively in the phase of the amplitude ϱ rather than in cross-sections.

In this paper we present a measurement of the ϱ-value at seven $\bar{p}$ momenta in the region between 181 and 590 MeV/c. The ϱ-value was derived from the differential elastic cross-sections by the Coulomb–nuclear interference method. In the analysis, only the data from the present experiment were used in order to determine the correlated parameters in a self-consistent way. The experiment was performed at the LEAR facility of CERN.

2. EXPERIMENTAL METHODS

The details of the experimental apparatus are described elsewhere [9]. Antiprotons were extracted from LEAR at fixed momenta: 609, 309, and 202 MeV/c. The beam was first focused 20 m upstream of the target, where a plastic scintillation counter for the time of flight (F1) and a momentum degrader were placed. The beam momentum was adjusted by carbon or CH_2 degraders. A beam-defining counter (SD), 20 mm in diameter, was placed 85 cm in front of the target. The $\bar{p}$ beam which passed SD then entered a 1 m diameter vacuum chamber. A second beam-defining counter (TD), 7 mm in diameter, was located 10 cm in front of the target at the centre of the vacuum chamber. The plastic scintillators of SD and TD were only 50 μm thick in order to minimize the multiple Coulomb scattering. A coincidence of SD and TD detectors limited the beam divergence to ±1.0° and the beam spot diameter to 5 mm.

A liquid-hydrogen target consisting of a vertical Mylar cylinder with 20 mm diameter and 40 mm height was used at the beam momenta of 500 and 590 MeV/c. A 7 mm thick liquid-hydrogen target with two windows glued on a steel frame of 20 mm diameter was used at 181 MeV/c. At the beam momenta between 219 and 287 MeV/c both targets were used, and cross-sections were compared in order to cross-check the thin-target thickness.

A cylindrical multiwire proportional chamber (MWPC) with a radius of 57.5 cm was placed around the target after the 250 μm thick Mylar window of the vacuum chamber. The MWPC covered angles in the range from 0° to ±75° in the horizontal plane and ±15° in the vertical direction. It had two wire planes which were inclined at ±12°. A 3 mm thick forward hodoscope (FHD) consisting of 32 slabs was placed just outside the MWPC. Each slab of the forward hodoscope covered 5° in the horizontal plane and ±15° in the vertical direction. An antineutron detector ring (ANC) surrounding the FHD served to measure the differential charge-exchange cross-sections. The upper (top) side, lower (bottom) side, and back of the vacuum chamber were covered with plastic scintillator hodoscopes (UHD, LHD, and BHD). These hodoscopes together with the forward hodoscope covered 73% of the full solid angle.

Data were taken at seven different $\bar{p}$ momenta between 181 and 590 MeV/c. At each of the seven beam momenta a total of 5×10^6 antiprotons were used for the measurement, and 5×10^4 elastic events were collected.

3. DIFFERENTIAL ELASTIC CROSS-SECTIONS

The first step of the analysis was to cut out the annihilation events in the target by use of the time of flight in FHD, UHD, LHD, and BHD. In the remaining events, elastically scattered antiprotons were identified in the forward hodoscope by their time of flight and their energy loss. A corresponding hit in the MWPC was required for each event. The full-to-empty-target ratio was about 10 at angles larger than 10° and 5 in the Coulomb–nuclear interference region.

Differential cross-sections have been deduced after a correction of the acceptance of the forward hodoscope which reached a maximum of 86% at 12° and then decreased to 13% at 75° in the laboratory frame. In addition, the efficiency of the MWPC was measured to be 99 ± 0.5%. The absorption of scattered antiprotons by the Mylar window of the vacuum chamber and the MWPC (altogether 500 μm thick) amounted to 0.15–2.5%, depending on the beam momentum and the scattering angle. An example of the differential cross-section at an $\bar{p}$ momentum of 287 MeV/c is shown in fig. 1a.

An essential point of the data analysis was the understanding of the effect of the multiple Coulomb scattering of antiprotons in the target. Calculations of the Rutherford scattering (single scattering) and the Molière scattering (multiple scattering) from the hydrogen target underestimated the forward differential cross-section, as shown in fig. 1b, when the beam divergence was not taken into account. The beam divergence was measured with the MWPC and was found to be 0.7° (r.m.s.) at 181 MeV/c. The Molière scattering, folded with this beam divergence, reproduced the data excellently. In the analysis we used the data at angles outside the multiple Coulomb scattering region at all momenta so that the analysis was free from the perturbation due to the multiple Coulomb scattering.

4. FITS TO THE CROSS-SECTIONS

The differential cross-sections were fitted using the following standard formulae [10]:

$$d\sigma/dt = d\sigma_C/dt + d\sigma_I/dt + d\sigma_N/dt , \tag{1}$$

where

$$d\sigma_C/dt = 4\pi(\alpha\hbar c/\beta t)^2 F(t)^2 , \tag{2}$$

$$d\sigma_I/dt = (\sigma_{tot}/\beta t)F(t) \exp(-\tfrac{1}{2}bt)(\varrho \cos\delta - \sin\delta) , \tag{3}$$

$$d\sigma_N/dt = (\sigma_{tot}/4\hbar c\sqrt{\pi})^2 (1 + \varrho^2) \exp(-bt) , \tag{4}$$

$$F(t) = (1 + t/0.71)^{-4} , \tag{5}$$

$$\delta(t) = -[\ln(9.5t) + 0.5772]\alpha/\beta . \tag{6}$$

Here, α is the fine-structure constant, β the velocity of the antiproton in the laboratory frame, F(t) the electromagnetic form factor of the proton, $\delta(t)$ the phase of the Coulomb amplitude [11], and $-t$ the four momentum transfer in units of $(GeV/c)^2$. There are three free parameters: σ_{tot}, ϱ, and b.

The best-fit parameters are listed in table 1. In fig. 2 the present results are plotted together with those from refs. [3], [4], and [6]. The present data agree with others in the range between 500 and 590 MeV/c. Below 500 MeV/c the ϱ-value decreases and reaches a minimum at about

260 MeV/c (E_{cm} = 18 MeV or $\sqrt{s}$ = 1894 MeV). At lower momenta it increases and reaches zero or even positive values at 220 MeV/c.

To test the stability of the fit, we changed σ_{tot} by +4% (4.5 mb) at 287 MeV/c and fitted the other two parameters to the data. The ϱ-value changed by −0.03 and b changed by +3.6 $(GeV/c)^{-2}$. On the other hand, the χ^2/DF increased to as much as 4.2.

Next we tested the effect of the spin dependence [10]. For this, the $d\sigma_N/dt$, defined by eq. (4), has to be replaced by

$$d\sigma_N/dt = (\sigma_{tot}/4\hbar c\sqrt{\pi})^2(1 + \varrho^2)(1 + \eta^2)\exp(-bt)\,. \tag{7}$$

Here η is the spin-dependent parameter, defined as

$$\eta^2 = (2|\Phi_2|^2 + |\Phi_3 - \Phi_1|^2)/|\Phi_1 + \Phi_3|^2\,, \tag{8}$$

where $\Phi_{1,2,3}$ are helicity amplitudes. Using this expression for $d\sigma_N/dt$, the three parameters σ_{tot}, ϱ, and b were fitted to the data at different fixed η-values ranging from 0 to 0.6 as shown in fig. 3. The χ^2/DF is close to 1.0 and does not change, indicating that η cannot be determined even with very precise data . Also the ϱ-value stays nearly constant, and σ_{tot} has a negative correlation with η. So we conclude that the correlation between ϱ and η is weak, which contradicts the results of ref. [12].

In the standard formulae, eqs. (1)–(6), the Coulomb-distortion effect on the waves of interacting particles is taken into account by the Coulomb phase [11]. We have done an independent test of the Coulomb-distortion effect using an optical model with a real and an imaginary potential of the Woods–Saxon type [13]. In the presence of the Coulomb interaction, the potential parameters were fitted to the forward differential cross-sections. When the Coulomb interaction was switched off, the ϱ-value calculated with these potential parameters changed only by 0.01. In the process of making these calculations we found rather general features of the potentials which give good fits to the data: the real potential has a larger range than the imaginary potential. For example, the real potential has a range of 2 fm and a depth of 60 MeV. The imaginary potential reaches 100 MeV at the distance of 1 fm at which the main damping of the incoming wave occurs. These general features do not depend on particular choices of the parameter set.

To conclude, we have presented the measurement of the ϱ-value down to 181 MeV/c for the first time. An oscillatory behaviour of the ϱ-value was found below 300 MeV/c. At present it is not clear whether dispersion relation calculations with poles in the unphysical region could reproduce it, or whether it is an indication of a $\bar{p}p$ resonant state above the threshold. Furthermore, the effect of the $\bar{n}$ threshold at 2.6 MeV (100 MeV/c) above the $\bar{p}p$ threshold should be considered as a possible source of this ϱ behaviour.

We wish to thank the LEAR machine group for their efforts and devotion to produce the high-quality beam of low-energy antiprotons which was the prerequisite for this experiment. The skilful designing and manufacturing of the liquid-hydrogen targets by the CERN cryotarget group are gratefully acknowledged. We also thank J. Ciborowski for his help in the early stage of this experiment.

REFERENCES

[1] W. Grein, Nucl. Phys. **B131** (1977) 255.
W. Grein, Proc. 4th European Antiproton Symp., Barr, 1978 (Centre National de la Recherche Scientifique, Paris, 1979), Vol. 1, p. 35.

[2] H. Kaseno, Nuovo Cimento **43A** (1978) 119.

[3] H. Kaseno et al., Phys. Lett. **61B** (1976) 203 and **68B** (1977) 487 (E).

[4] H. Iwasaki et al., Phys. Lett. **103B** (1981) 247.

[5] H. Iwasaki et al., Nucl. Phys. **A433** (1985) 580.

[6] M. Cresti, L. Peruzzo and G. Sartori, Phys. Lett. **132B** (1983) 209.

[7] V. Ashford et al., Phys. Rev. Lett. **54** (1985) 518.

[8] L.N. Bogdanova, O.D. Dalkarov and I.S. Shapiro, Ann. Phys. **84** (1974) 261.
G.C. Rossi and G. Veneziano, Phys. Rep. **63** (1980) 153.

[9] W. Brückner et al., Proc. 7th European Symp. on Antiproton Interactions, Durham, 1984 (Inst. Phys. Conf. Ser. No. 73, Adam Hilger Ltd., Bristol and Boston, 1985), p. 157.
W. Brückner et al., technical report, in preparation.

[10] C. Bourrely, J. Soffer and D. Wray, Nucl. Phys. **B77** (1974) 386.

[11] M.P. Locher, Nucl. Phys. **B2** (1967) 525.

[12] M. Lacombe et al., Phys. Lett. **124B** (1983) 443.

[13] E.H. Auerbach, Comput. Phys. Commun. **15** (1978) 165.

Table 1

Result of the fits

Momentum (MeV/c)	Momentum full width (MeV/c)	ϱ	σ_{tot} (mb)	b $(GeV/c)^{-2}$	χ^2/DF	DF
590	10	0.203 ± 0.110	140.0 ± 2.6	22.8 ± 0.94	1.18	49
505	10	−0.046 ± 0.119	162.7 ± 2.6	26.4 ± 1.14	1.45	48
287	14	−0.103 ± 0.018	229.3 ± 2.0	32.3 ± 1.70	1.04	39
261	18	−0.142 ± 0.026	252.4 ± 2.0	39.2 ± 2.00	1.06	39
239	23	−0.028 ± 0.032	261.2 ± 5.7	52.4 ± 3.80	1.31	46
219	8	0.093 ± 0.098	292.1 ± 23.6	61.2 ± 16.5	0.78	41
181	16	0.100 ± 0.084	339.4 ± 30.6	83.7 ± 24.0	0.91	43

Figure captions

Fig. 1 a) The differential elastic cross-section at 287 MeV/c. A best-fit curve as well as two other curves with σ_{tot} and b from the best fit and with $\varrho = \pm 1$ are shown.
b) The differential elastic cross-section at very forward angles at 181 MeV/c. The deviation of the calculations from the data at angles larger than 7° is due to the strong interaction.

Fig. 2 Real-to-imaginary ratios of the $\bar{p}p$ forward elastic-scattering amplitude. The data of refs. [3], [4], and [6] are included. A curve of the dispersion relation calculation without additional pole terms and the best-fit curve of Iwasaki et al. [4, 5] with a pole term are also shown.

Fig. 3 Effects of the spin-dependent parameter η at 287 MeV/c; σ_{tot}, ϱ, and b are fitted to the data at fixed η-values between 0 and 0.6.

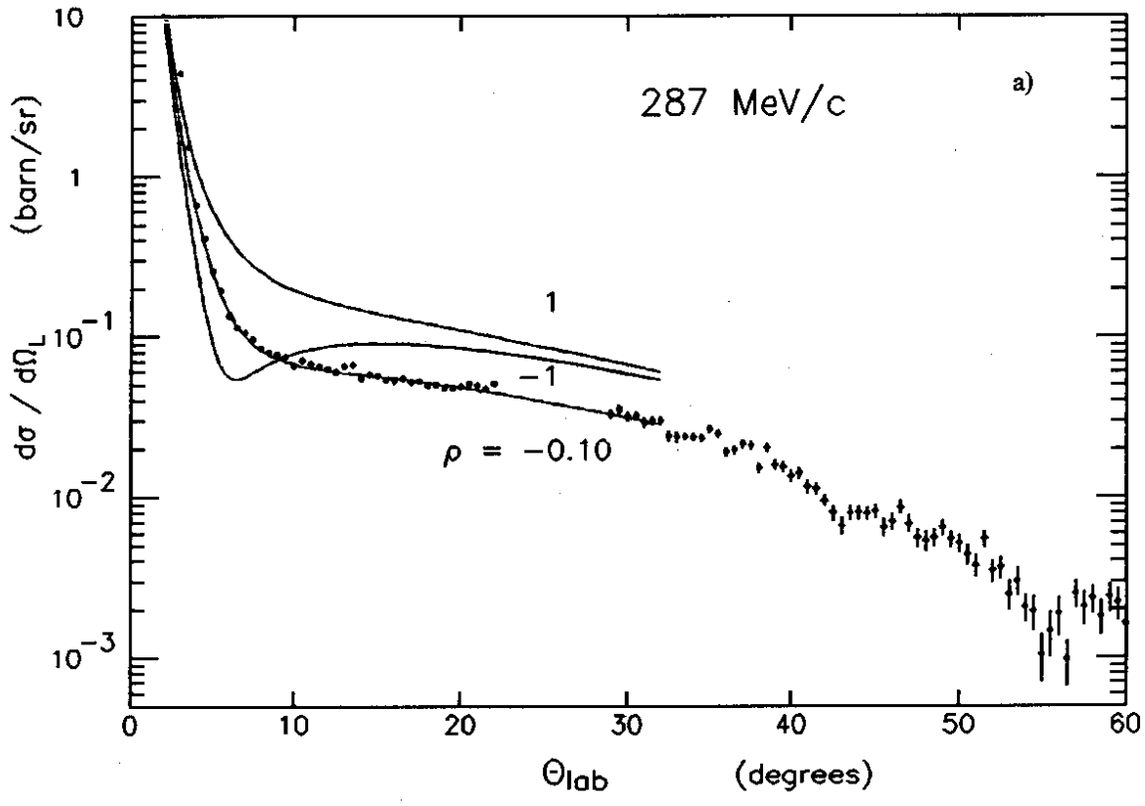
287 MeV/c
a)
1
−1
ρ = −0.10
dσ / dΩL (barn/sr)
Θlab (degrees)

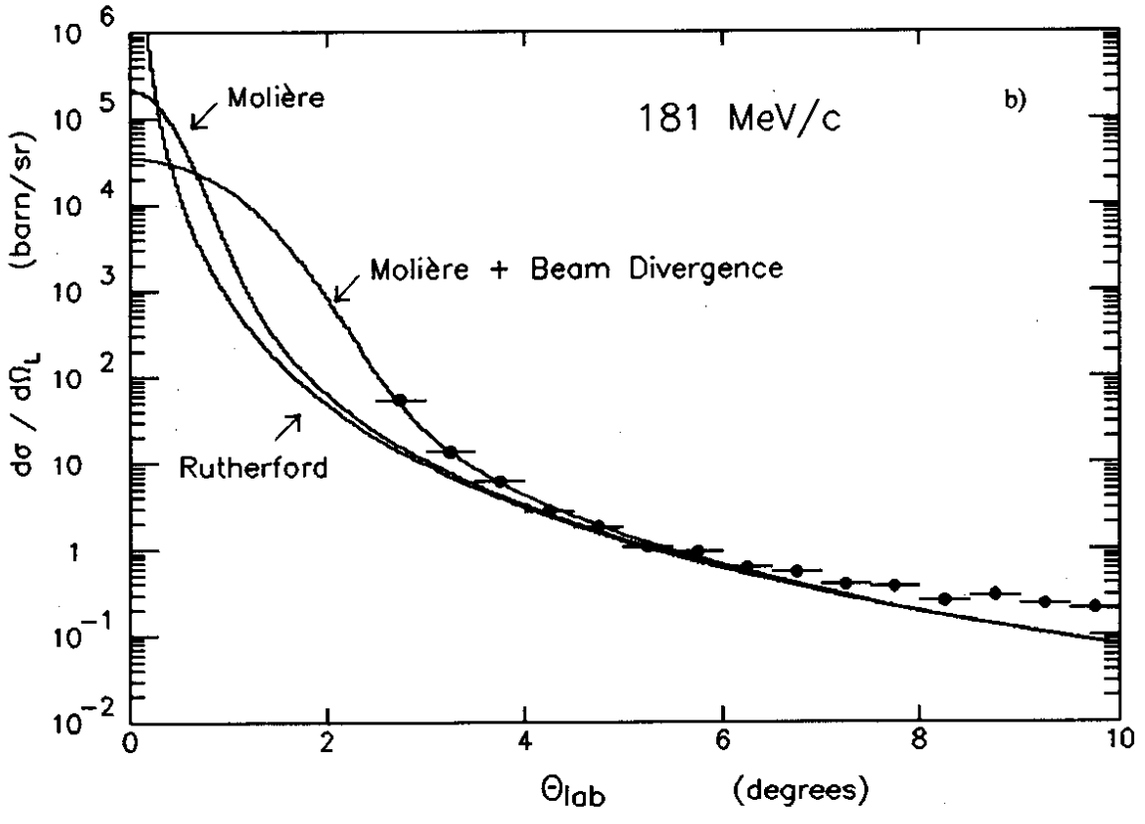
181 MeV/c
b)
Molière
Molière + Beam Divergence
Rutherford
dσ / dΩL (barn/sr)
Θlab (degrees)

Fig. 1

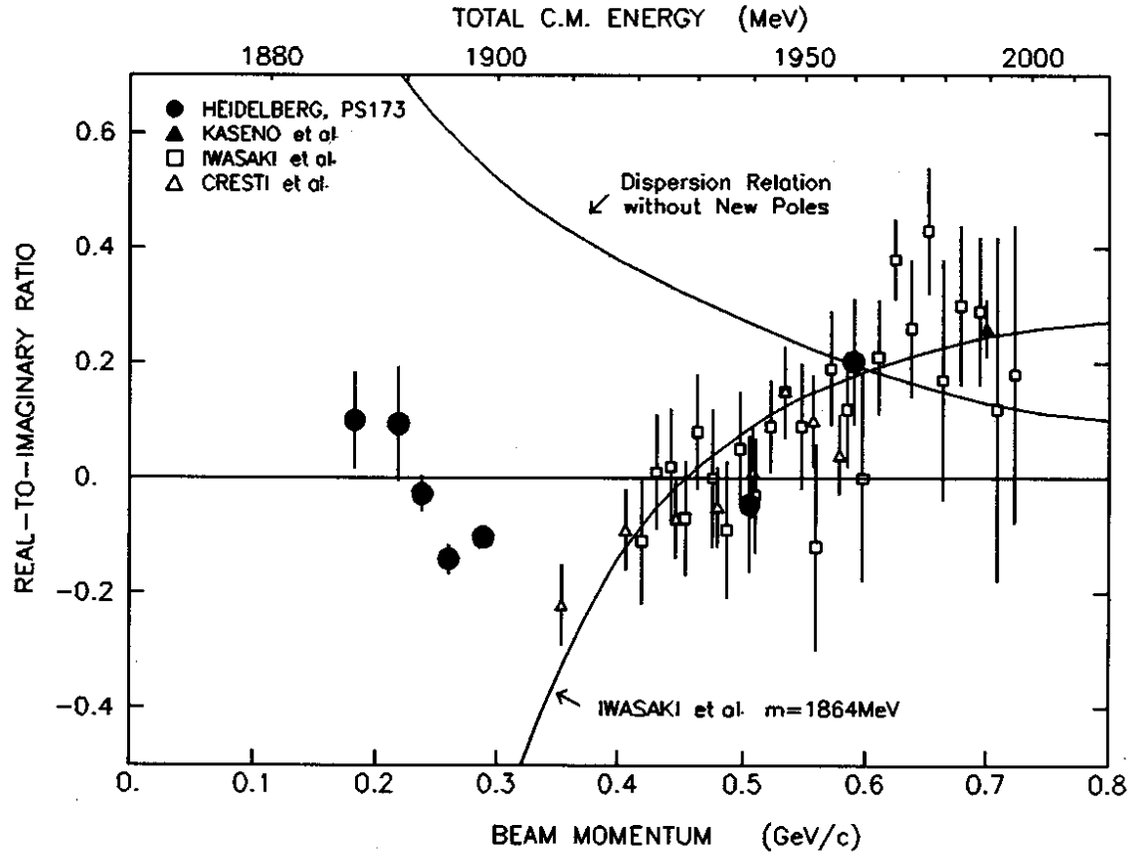
TOTAL C.M. ENERGY (MeV)
1880
1900
1950
2000
HEIDELBERG, PS173
KASENO et al.
IWASAKI et al.
CRESTI et al.
Dispersion Relation
without New Poles
IWASAKI et al. m=1864MeV
REAL-TO-IMAGINARY RATIO
BEAM MOMENTUM (GeV/c)
0.6
0.4
0.2
0.
-0.2
-0.4
0.1
0.3
0.5
0.7
0.8

Fig. 2

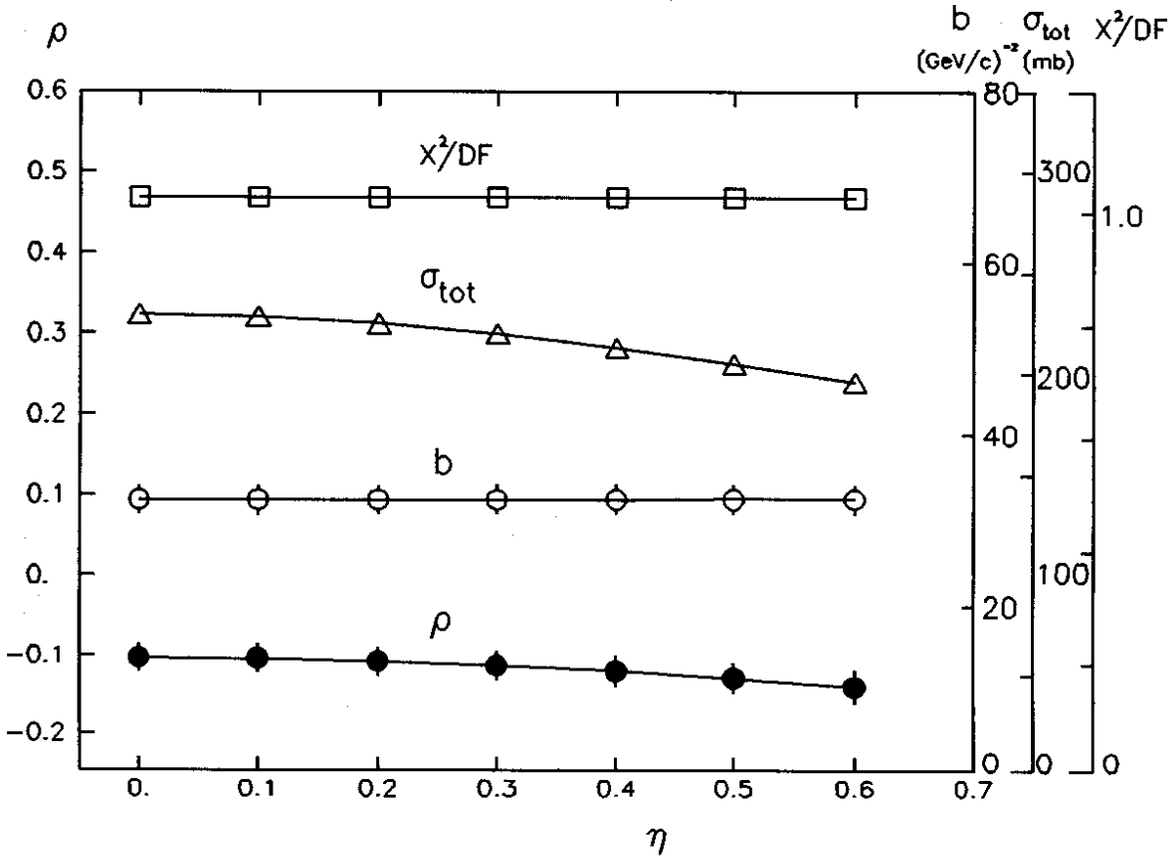
ρ
b
(GeV/c)^-2
σtot
(mb)
X²/DF
X²/DF
σtot
b
ρ
η
0.6
0.5
0.4
0.3
0.2
0.1
0.
-0.1
-0.2
80
60
40
20
0
300
200
100
1.0
0.1
0.2
0.3
0.4
0.5
0.6
0.7

Fig. 3